Glycoconjugate Journal 17, 877–885, 2000

The N-glycan acceptor specificity of a glucuronyltransferase, GlcAT-P, associated with biosynthesis of the HNK-1 epitope

Shogo Oka[1], Koji Terayama[1], Kimiyuki Imiya[1], Shoji Yamamoto[1], Akihiro Kondo[2], Ikunosin Kato[2] and Toshisuke Kawasaki[1]*

[1] *Department of Biological Chemistry and CREST (Core Research for Educational Science and Technology) Project, Japan Science and Technology Corporation, Graduate School of Pharmaceutical Sciences, Kyoto University, Kyoto 606-8501, Japan,* [2] *Biotechnology Research Laboratories, TAKARA SHUZO Co., Ltd., Shiga, Japan*

The acceptor specificity of a rat brain glucuronyltransferase, GlcAT-P, associated with biosynthesis of the HNK-1 epitope on glycoproteins, was investigated using asialoorosomucoid as a model acceptor substrate. Structural analysis of N-linked oligosaccharides, to which glucuronic acid was transferred by GlcAT-P, by means of two-dimensional mapping of pyridylamino-oligosaccharides and MS spectrometry, demonstrated that the enzyme transferred glucuronic acid to bi-, tri-, and tetra-antennary complex type sugar chains, with almost equal efficiency, indicating that the enzyme has no preference as to the number of acceptor sugar branches. Next, we studied the branch specificity of this enzyme by means of the selective branch scission method involving two step exoglycosidase digestion using authentic pyridylamino-oligosaccharides. The GlcAT-P is highly specific for the terminal *N*-acetyllactosamine structure and no glucuronic acid was incorporated into a Galβ1-3GlcNAc moiety. The GlcAT-P transferred glucuronic acid to the galactose residues in the *N*-acetyllactosamine branches of bi-, tri-, and tetra-antennary oligosaccharide chains, with different efficiencies and most preferentially to those in the Galβ1-4GlcNAcβ1-4Manα1-3 branch.

Keywords: **HNK-1 epitope, glucuronyltransferase (GlcAT), asialo-orosomucoid (ASOR), branch specificity**

Introduction

The HNK-1 carbohydrate epitope, recognized by monoclonal antibody HNK-1 [1], is characteristically expressed in the mammalian central and peripheral nervous systems, and this expression is temporally and spatially regulated during development [2,3]. The epitope has been found on many neural cell adhesion molecules, such as neural cell adhesion molecule (N-CAM), L1, J1, myelin-associated glycoprotein (MAG), transiently expressed axonal glycoprotein-1 (TAG-1), and P0, and proteoglycans [4–7]. Recent studies on HNK-1 reactive carbohydrates suggested that this epitope plays important roles in cell-to-cell interaction events, such as cell adhesion, migration, and neurite outgrowth [8–10]. This epitope is expressed not only on glycoproteins but also on glycolipids [11]. The structure of the HNK-1 epitope has been demonstrated to be the sulfated trisaccharide SO_4-3GlcAβ1-3Galβ1-4GlcNAc, which is shared by glycolipids and glycoproteins [12–14]. Because the inner structure, Galβ1-4GlcNAc, is commonly found in various glycoproteins and glycolipids, glucuronyltransferases are key enzymes in the biosynthesis of the HNK-1 epitope.

We previously showed that there are two types of glucuronyltransferase activities associated with the biosynthesis of the HNK-1 epitope in rat brain; one for glycoprotein acceptors (GlcAT-P) such as asialoorosomucoid (ASOR) [15], and the other for glycolipid acceptors (GlcAT-L) such as synthetic glycolipid nLc-PA14 [16]. We had previously purified the GlcAT-P to homogeneity from postnatal day 14 rat brain [17] and cloned its cDNA [18]. Using the GlcAT-P cDNA as a probe, a second glucuronyltransferase (GlcAT-S(D)) involved in the biosynthesis of the HNK-1 carbohydrate epitope had been cloned [19,20]. The GlcAT-P is highly specific for the terminal *N*-acetyllactosamine structure, Galβ1-4GlcNAc [17], although the enzyme has been reported to have a little glucuronyltransferase activity towards the core oligosaccharide of glycosaminoglycan-protein linkage

*To whom correspondence should be addressed: Toshisuke Kawasaki, Tel.: + 81-75-753-4572; Fax: +81-75-753-4605; E-mail: kawasaki@pharm.kyoto-u.ac.jp

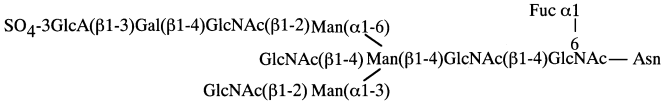

Figure 1. Structure of the HNK-1 carbohydrate epitope on P0 glycoprotein.

region [21,22]. It should be noted that the *N*-acetyllactosamine structure is ubiquitously present in many different types of sugar chains. For example, ASOR, which is used as a conventional substrate for GlcAT-P, contains bi-, tri-, and tetra-antennary *N*-glycoside type sugar chains, all of which bear the *N*-acetyllactosamine structure on each branch [23]. Until now, structural information with regards to the HNK-1epitope on N-glycan is very limited. The HNK-1 carbohydrate epitope on P0 glycoprotein had been determined as shown in Figure 1 [14] and the same structure was found on PASII/PMP22 [24]. This may suggest that GlcAT-P recognizes a particular type of sugar chain and transfers glucuronic acid to the branches. In this study, we attempted to determine whether or not there is some specificity in the transfer of GlcA with regard to the type of sugar chains and/or the branch on the sugar chains using ASOR and authentic pyridylamino-oligosaccharides as model acceptor substrates.

Materials and methods

Materials

UDP-[^{14}C] glucuronic acid was purchased from ICN Radiochemicals (CA, USA). Orosomucoid was provided by Dr. M. Wickerhauser of the American Red Cross Research Center, Bethesda, MD. Asialoorosomucoid (ASOR) was prepared by hydrolysis of orosomucoid in 0.05 M H_2SO_4 at 80°C for 1 h as described previously [15]. *N*-Glycosidase-F was obtained from Boehringer Mannheim Biochemica. *β*-Glucuronidase (bovine liver) was from Seikagaku Corporation (Tokyo, Japan). *β*-Galactosidase inhibitor was kindly provided by Nippon Shinyaku (Kyoto, Japan). The several PA-oligosaccharides used in this study were provided by TaKaRa Shuzo, Co., Ltd (Kyoto, Japan) (see Figure 2). A TaKaRa GlycoSEQ^{TM} kit, which had been modified to include *β*-glucuronidase, and HPLC columns of TaKaRa Palpak Type, N and R were kindly provided by TaKaRa Shuzo Co., Ltd. The GlcAT-P used in this study was purified from rat brain according to the procedure described previously [17].

Preparation of pyridylaminated-oligosaccharides

ASOR (180 mg) was coupled with cyanogen bromide-activated Sepharose 4B (10 ml; Pharmacia Uppsala, Sweden) according to the manufacturer's manual. An aliquot of ASOR-Sepharose 4B was incubated with the purified GlcAT-P in the presence of UDP-[^{14}C] glucuronic acid under the conditions described

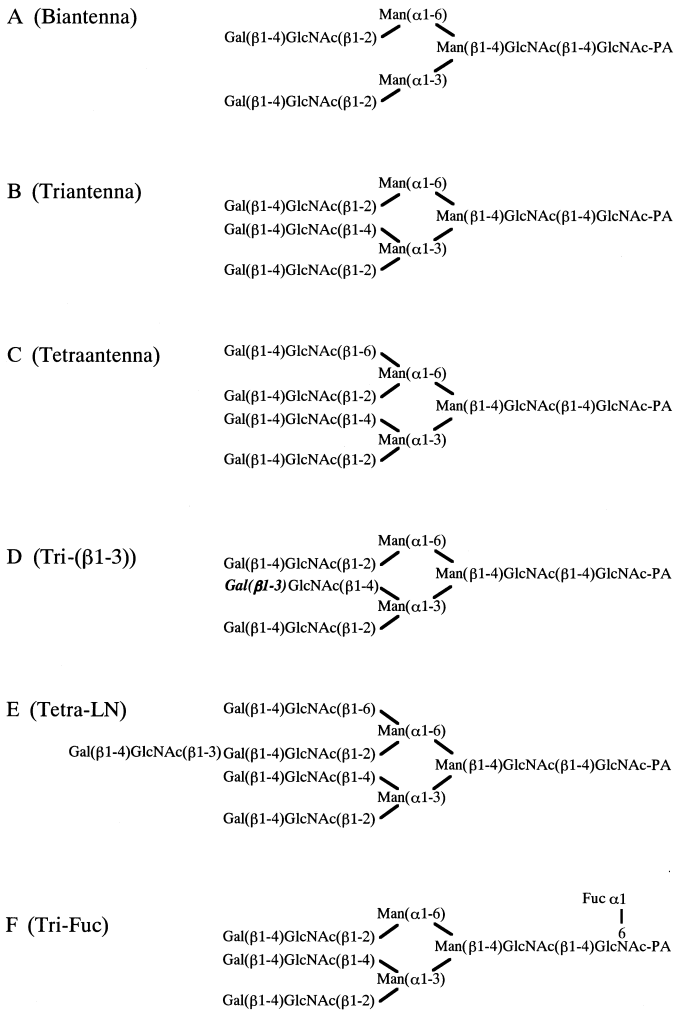

Figure 2. Structures of the PA-oligosaccharides used as substrates to examine the acceptor specificity of GlcAT-P and as standards for two-dimensional mapping analysis.

previously [15,17]. After incubation at 37°C overnight, the resin was collected by centrifugation and washed with 0.5 ml of 0.5% SDS eight times until radioactivity was not detected in the supernatant. To release the oligosaccharides from ASOR, the [^{14}C] glucuronic acid-transferred ASOR-Sepharose 4B was digested with *N*-glycosidase-F according to the procedure described previously [15]. Ninety percent of the incorporated radioactivity was released from the ASOR-Sepharose 4B. The supernatant was lyophilized and then subjected to gel filtration on Sephadex G-25 (1.0 × 10 cm), which had been equilibrated with pyridine-acetate buffer, pH 5.0. The void volume fractions containing the oligosaccharides were pooled and lyophilized. The oligosaccharides were pyridylaminated with 2-aminopyridine using a TaKaRa Palstation Model 4000 according to the manufacturer's manual. The reaction mixture was subjected to gel filtration on a column of TSK-gel G-2500 PW XL in a Shimadzu LC-9A chromatograph. The column was eluted with 10 mM CH_3COO-NH_4 buffer, pH 6.0, at the flow rate of

2 ml/min. The labeled oligosaccharides were eluted near the void volume (retention time, 5–10 min).

Anion exchange chromatography

The lyophilized void volume fraction from the TSK-gel G-2500 PW XL column was dissolved in a small volume of water and then applied to a TSK-gel DEAE 5PW (7.5 × 75 mm) anion exchange HPLC column. Elution was performed at the flow rate of 1 ml/min using two solvents, A and B. Solvent A was water (pH adjusted to 9.0 with ammonium hydroxide) and solvent B was 0.25 M ammonium acetate buffer, pH 8.0. The column was equilibrated with solvent A. After injection of a sample, the concentration of solvent B was increased linearly to 50% in 10 min and then maintained (50%) for 25 min. PA-oligosaccharides were detected with excitation at 310 nm and emission at 380 nm. The PA-oligosaccharides bearing GlcA were eluted in the second (R1) and third (R2) peaks following the neutral PA-oligosaccharides peak (see Figure 3A).

β-Glucuronidase digestion

The radio-labeled PA-oligosaccharides obtained above were dissolved in 400 µl 10 mM sodium acetate buffer, pH 3.8, containing 45 mU of β-glucuronidase and 100 µg of β-galactosidase inhibitor. The reaction mixture was incubated at 37°C overnight. After stopping the reaction by the addition of 400 µl of ethanol, the mixture was incubated on ice for 15 min and then centrifuged at 10,000 × g for 10 min. The supernatant was fractionated on Sephadex G-25 (1.0 × 10 cm). An aliquot of each fraction was used to measure ^{14}C-radioactivity and fluorescence intensity. The void volume fractions were pooled and used for the following analysis.

Two-dimensional mapping of PA-oligosaccharides

The void volume fraction obtained on β-glucuronidase digestion was subjected to reverse phase HPLC on a YMC-Pack ODS-AQ column (0.46 × 25 cm), which had been equilibrated with 0.1 M ammonium acetate buffer, pH 4.0. Elution of the column was carried out with a linear gradient of 0 to 0.5% n-butyl alcohol. PA-oligosaccharides were detected with excitation at 320 nm and emission at 400 nm. The materials obtained on reverse phase chromatography were then applied to a YMC-Pack PA column

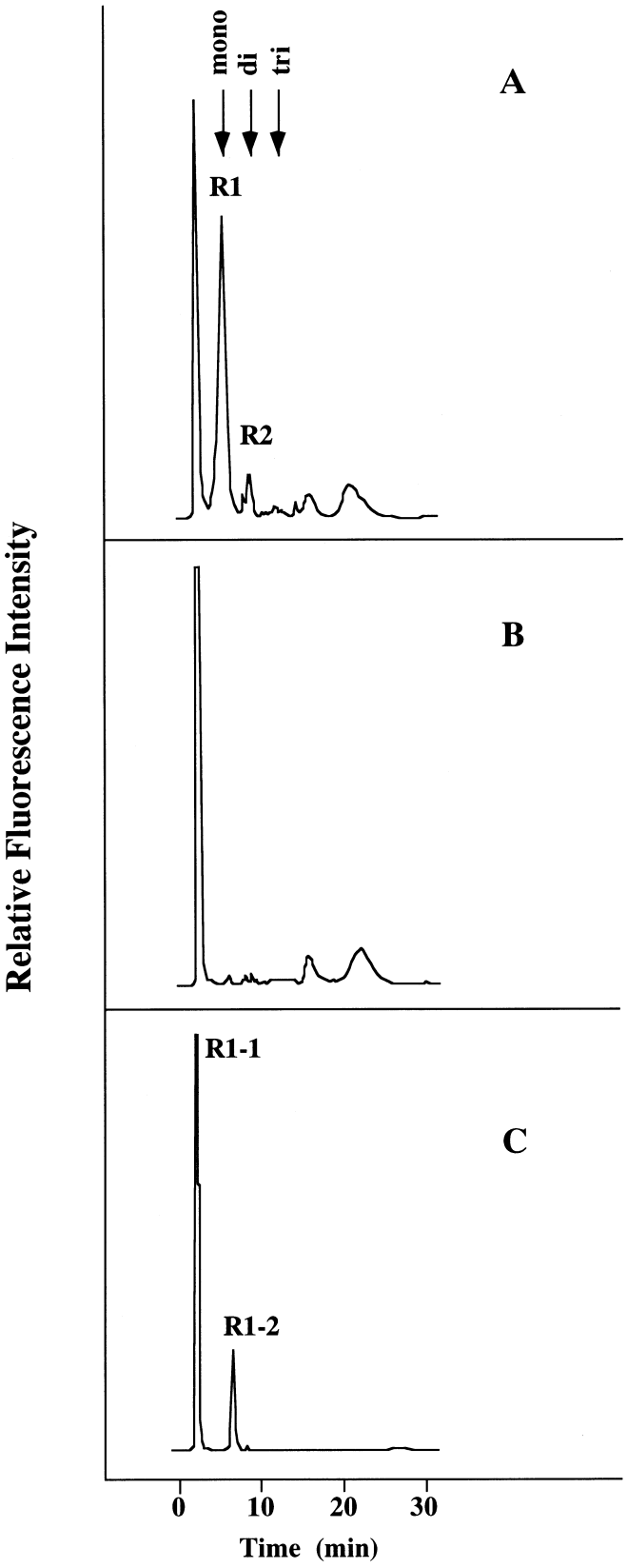

Figure 3. TSK-gel DEAE 5PW anion exchange chromatography. Oligosaccharides released from ASOR-Sepharose 4B, which had been incubated in the presence (A) or absence (B) of GlcAT-P under the conditions given under Materials and Methods, were pyridylaminated and then applied to a TSKgel DEAE 5PW column. Arrows indicate the elution positions of mono-, di-, and trisialo oligosaccharides. (C) The R1 fraction in (A) was digested with β-glucuronidase and then applied to a TSKgel DEAE 5PW column.

(0.46 × 25 cm), which had been equilibrated with 65% acetonitrile in 3% acetate-triethylamine buffer, pH 7.3. The column was eluted with a reverse linear gradient of 65% to 50% acetonitrile.

Mass spectrometric analysis of pyridylaminated oligosaccharides

The oligosaccharides were lyophilized and dissolved in 20 mM ammonium-acetate buffer, pH 4.0, containing 50% acetonitrile (10 pmol/μl), and then injected into a Perkin Elmer Sciex (Thornhill, Canada) API-III ion spray mass spectrometer (MS) with an atmospheric-pressure ionization ion source. The mass spectrometer was operated in the positive mode, the ion spray voltage was set to 5100 V, and the interface plate voltage was 650 V. The orifice voltage was 100 V. Scanning was carried out from m/z 800 to 2200, with a step size of 0.5 Da. A collisionally activated dissociation (CAD) spectrum was obtained with argon as the collision gas. A CAD daughter ion spectrum was recorded from m/z 50 to 2400.

Selective branch scission method

The authentic PA-oligosaccharides listed in Figure 2 were incubated with GlcAT-P under the standard conditions described previously [15,17] at 37°C for 3 h. The enzyme reaction was terminated by heating the reaction mixture at 100°C for 3 min. After centrifugation of the reaction mixture, the supernatant fraction was applied on a TSK-gel DEAE 5PW column to separate PA-oligosaccharides bearing GlcA. Structural analysis of PA-oligosaccharides by means of Selective Branch Scission Method was carried out with a TaKaRa GlycoSEQ^{TM} kit according to the manufacturer's manual. Approximately 20 pmol of PA-oligosaccharides bearing a single GlcA residue were dissolved in 20 μl of 250 mM citrate buffer, pH 5.0, containing *β-N*-acetylhexosaminidase and *β*-galactosidase. The reaction mixture was incubated at 37°C for 6 h. After inactivation of these enzymes by treatment at 100°C for 15 min, 2.5 μl each of *β*-galactosidase and *β*-glucuronidase were added to the mixture, followed by incubation at 37°C for 16 h. After boiling for 15 min, the reaction mixture was centrifuged at 10,000 × g for 5 min. The supernatant was applied to a TaKaRa Palpak Type R (0.46 × 25 cm) reverse phase HPLC column equilibrated with 0.1 M acetate-triethylamine buffer, pH 4.0, containing 0.005% n-butylalcohol at a flow rate of 1.0 ml/min. PA-sugars were detected with excitation at 320 nm and emission at 400 nm. The supernatant was also applied to a TaKaRa Palpak Type N (0.46 × 25 cm) normal-phase HPLC column using two solvent systems. Solvents A and B were 50 mM acetate-triethylamine buffer, pH 7.3, containing 75% and 50% acetonitrile, respectively. The column was equilibrated with 80% of solvent A and 20% of solvent B. The concentration of solvent B was linearly increased from 20% to 36% in 60 min at the flow rate of 1.0 ml/min. PA-sugars were detected with excitation at 310 nm and emission at 380 nm. The structures of the digested products were deduced from the elution times by comparing them with those of the standard PA-oligosaccharides listed in Figure 6.

Results

Analysis of glucuronic acid-bearing sugar chains

In order to analyze the carbohydrate structure, to which GlcA was transferred, the carbohydrates released from in vitro glucuronylated ASOR-Sepharose 4B by *N*-glycosidase F were labeled with 2-aminopyridine. Upon fractionation of the pyridylamino-labeled oligosaccharides on a TSK-gel DEAE-5PW column, two acidic fractions, R1 (second peak) and R2 (third peak), were obtained in addition to the passthrough (neutral) fraction (Figure 3A). The elution positions of R1 and R2 corresponded to those of mono- and di-sialo oligosaccharides, respectively. About 15% of the fluorescence and 85% of the radioactivity applied were recovered in the R1 fraction and about 2% of the fluorescence and 15% of the radioactivity in R2. These two acidic peaks were not detected for the control oligosaccharides prepared from ASOR-Sepharose 4B, which had been incubated in the absence of GlcAT-P (Figure 3B). This indicated that the oligosaccharides recovered in these two acidic fractions contained transferred glucuronic acid. The major peak (R1) was subjected to further analysis. The R1 fraction was digested with *β*-glucuronidase in the presence of a *β*-galactosidase inhibitor, which is necessary to inhibit the contaminating *β*-galactosidase in the *β*-glucuronidase used, and then the reaction mixture was applied to a TSK-gel DEAE-5PW column again (Figure 3C). Approximately 85% of the oligosaccharides applied were detected in the unretained (neutral) fraction (R1-1) as a result of the release of glucuronic acid, which was confirmed by the absence of ^{14}C-radioactivity in the R1-1 fraction.

Analysis of the R1-1 fraction was carried out by two-dimensional mapping of PA-oligosaccharides. The first dimension comprised reverse phase HPLC with a YMC-Pack ODS-AQ column and the second dimension with a YMC-Pack PA column. As shown in Figure 4A, the R1-1 fraction was separated into two major fractions (R1-1-1 and R1-1-2) on the first column (YMC-Pack ODS-AQ). Upon fractionation of the second column (YMC-Pack PA), the R1-1-1 fraction was separated into two major peaks (R1-1-1-1 and R1-1-1-2), the elution positions of which corresponded well with those of bi- and tetra-antennary oligosaccharides, respectively (Figure 4Ba). The R1-1-2 fraction gave a single peak (R1-1-2-1), the elution position of which corresponded with that of tri-antennary oligosaccharide (Figure 4Bb).

In order to confirm the structures of these oligosaccharides, mass spectrometry (MS) was carried out. The results for the R1-1-1-2 fraction are shown in Figure 5. The R1-1-1-2 fraction gave rise to a doubly charged molecular ion at m/z 1225.8. MS/MS analysis of this peak gave rise to fragment

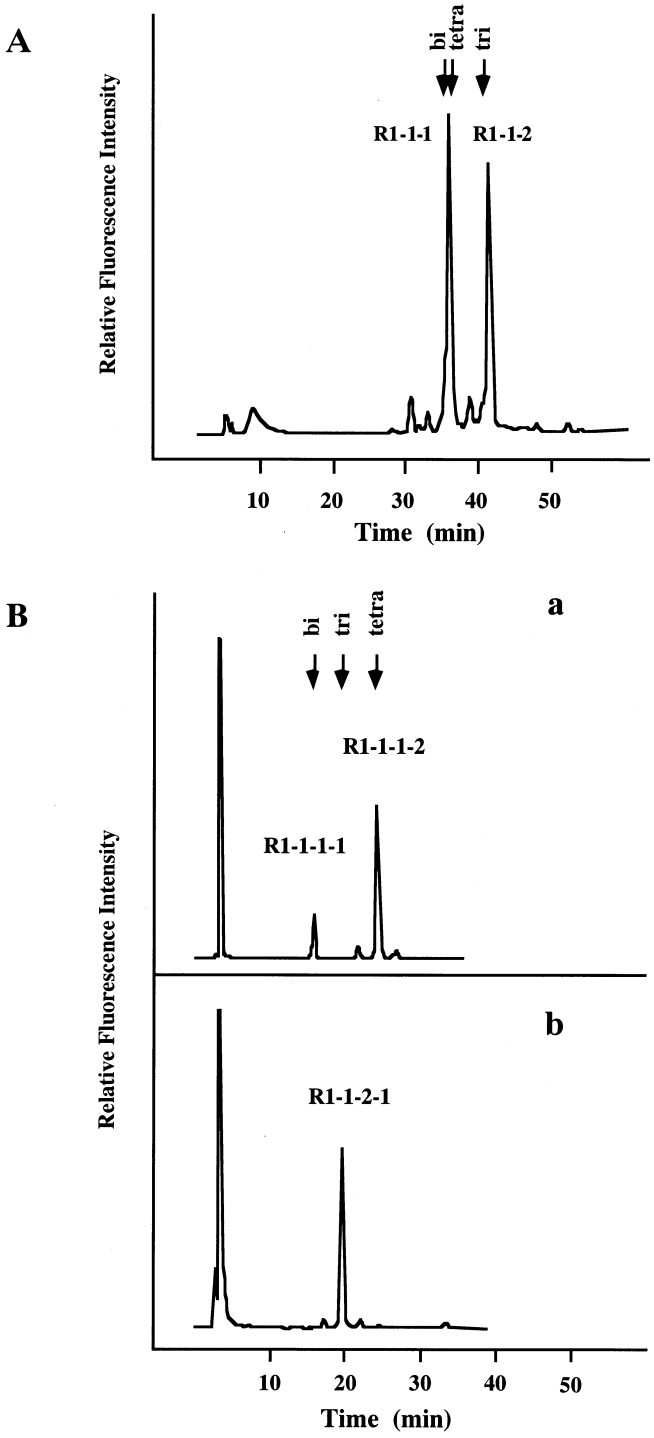

Figure 4. Two-dimensional mapping of PA-oligosaccharides. (A) The R1-1 fraction in Figure 2C was applied to a YMC-Pack ODS AQ reverse phase column. (B) The R-1-1-1 (a) and R1-1-2 (b) fractions were applied to a YMC-Pack PA size-fractionation column. Arrows indicate the elution positions of the authentic bi-, tri-, and tetra-antennary oligosaccharides sugar chains shown in Figure 2.

ions at m/z 2288.6, 2085, 1923.4, 1720.8, 1557.6, 1191.2, and 1044.2, which are consistent with the loss of successive monosaccharide residues from the molecular ion. The signals at m/z 893.4 and 366 indicated the presence of fragments containing *N*-acetyl glucosamine (GlcNAc)-GlcNAc-hexose-hexose-hexose and GlcNAc-hexose, respectively. These results confirmed that the R1-1-1-2 fraction has the structure of a tetra-antennary oligosaccharide, as shown in Figure 2C. The same analysis was carried out for the R1-1-2-1 fraction (data not shown), which confirmed that this fraction has the structure of a tri-antennary oligosaccharide, as shown in Figure 2B.

These results indicated that there is no bias as to which class (bi-, tri- or tetra-antennary) of oligosaccharides the GlcA is transferred to. Thus, 10.9% of the GlcA transferred was present in biantennary, 44.0% in triantennary and 45.1% in tetraantennary oligosaccharides. These percentages correspond almost exactly to the respective percentage occurrence of these classes of oligosaccharides (10.0%, 39.1% and 42.6%) in native human orosomucoid [23,25].

Analysis of glucuronic acid carrying sugar branches

In the next experiment, we investigated whether or not there is any specific branch to which glucuronic acid is preferentially transferred. We used the authentic PA-oligosaccharides listed in Figure 2 as substrates with incubation with GlcAT-P for 3 h. In the case of tri (β1-3), the PA-oligosaccharides were incubated with GlcAT-P for 16 h in order to determine whether or not GlcA is transferred to the Galβ1-3GlcNAc branch. The reaction products were applied to a TSK-gel DEAE-5PW column under the same conditions as in Figure 3. The percentage of GlcA transferred to each type of oligosaccharide was estimated from each peak area and the results are presented in Table 1. Similar amounts of GlcA were transferred to bi-, tri-, tetra-, and tetra + LN oligosaccharides (16.1% to 27.0%), confirming, as described above, that GlcAT-P almost equally transfers to these sugar chains. The mono-glucuronylated PA-oligosaccharides were collected and subjected to the Selective Branch Scission Method with a modified TaKaRa GlycoSEQ^{TM} kit. The principle of this method is as follows: when oligosaccharides bearing glucuronic acid are digested with reagent A containing β-*N*-acetylhexosaminidase and β-galactosidase, the galactose and *N*-acetylglucosamine residues in the terminal lactosamine structure are released, while those substituted with GlcA are not. The reaction products are subsequently treated with reagent B containing β-galactosidase and β-glucuronidase. Glucuronic acid and galactose are released from the branch to which glucuronic acid had been transferred and a GlcNAc residue remains on the branch. These digestion products were subjected to two-dimensional mapping and the structures of the oligosaccharides were deduced by comparison with the standard PA-oligosaccharides listed in Figure 6. Typical results of reverse phase HPLC are presented in Figure 7. Two, three, and four major peaks were detected for the digestive products of bi-, tri-, and tetra-antennary oligosaccharides, respectively. But, only two peaks

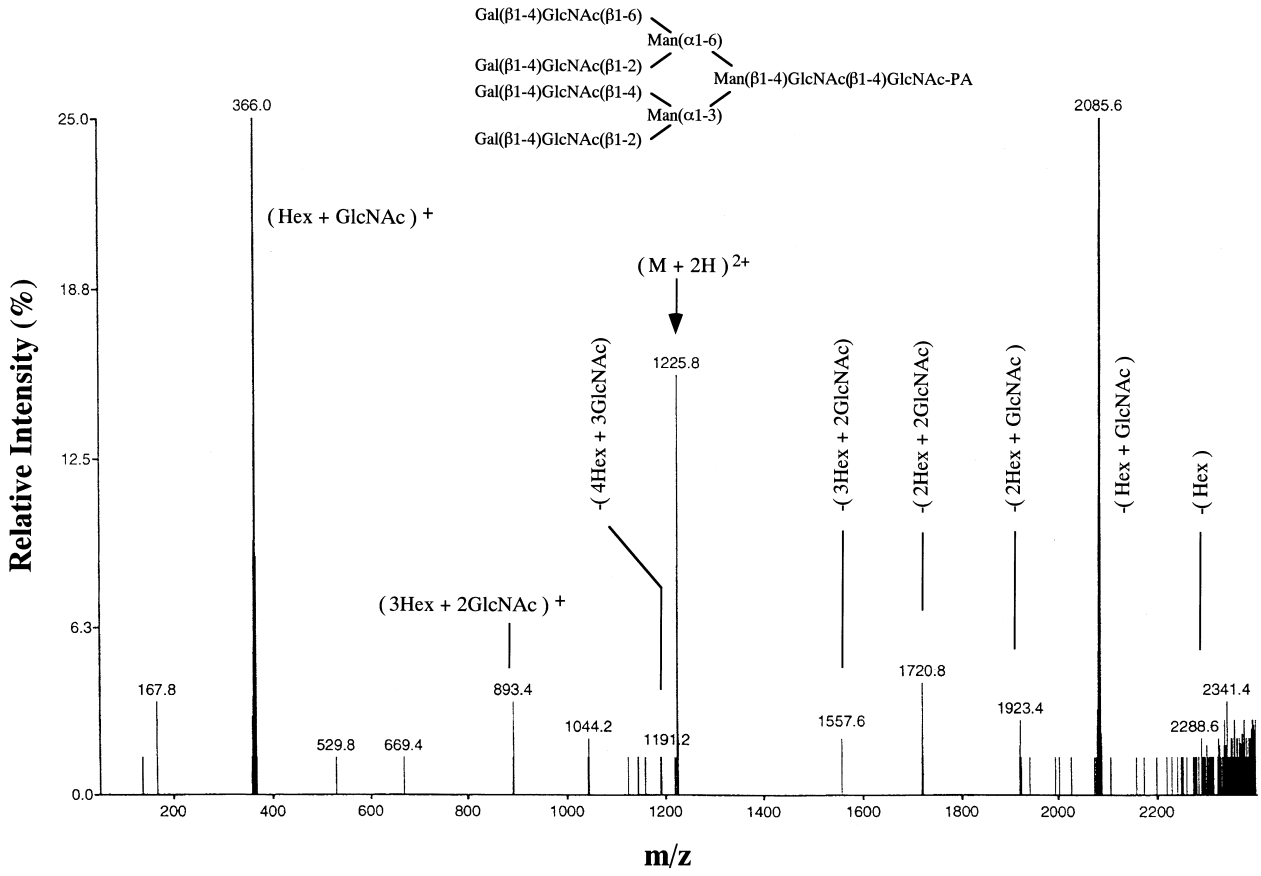

Figure 5. MS/MS spectrum from CAD of the doubly charged precursor ion (m/z 1225.8) of R1-1-1-2.

were detected in the case of Tri-(β1-3). All these peaks corresponded well with those of the standard PA-oligosaccharides listed in Figure 6. The proportion of GlcA transferred to each branch was estimated from each peak area and the results are summarized in Table 2. Sixty percent of the digestive product of bi-antennary oligosaccharides was

Table 1. Percentage distributions of GlcA-transferred oligosaccharides. The authentic PA-oligosaccharides (1 nmol each) listed in Figure 2 were incubated with GlcAT-P for 3 h. The reaction products were applied to a TSK-gel DEAE-5PW column and mono-, di-, and tri-GlcA transferred oligosacharides were estimated by each peak area. The proportion of the GlcA transferred oligosaccharides were represented by percentages of the oligosaccharide substrate used (1 nmol)

	Percentages of GlcA-transferred oligosaccharides			
PA-oligosaccharides	*mono*	*di*	*tri*	*total*
Biantenna	15.3	0.76	–	16.1
Triantenna	22.0	2.37	0.08	24.5
Tetraantenna	21.5	2.44	0.14	24.1
Tetra + LN	23.7	3.08	0.20	27.0
Tri(β1-3)[a]	40.1	11.4	–	51.5
Tri + Fuc[a]	39.6	20.1	3.9	63.6
Triantenna[a]	29.6	18.0	3.6	51.2

[a]Incubation was carried out for 16 h with GlcAt-P.

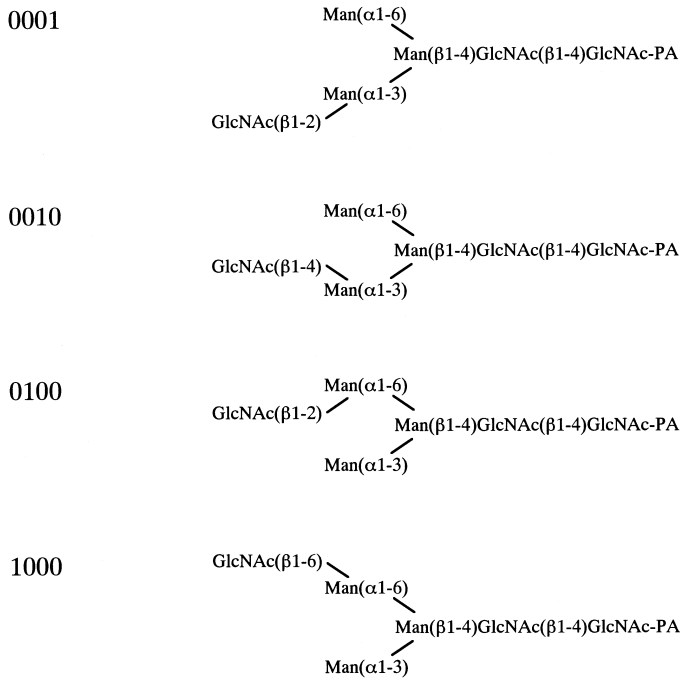

Figure 6. Structures of the PA-oligosaccharides used as standards for branch specificity analysis of GlcAT-P.

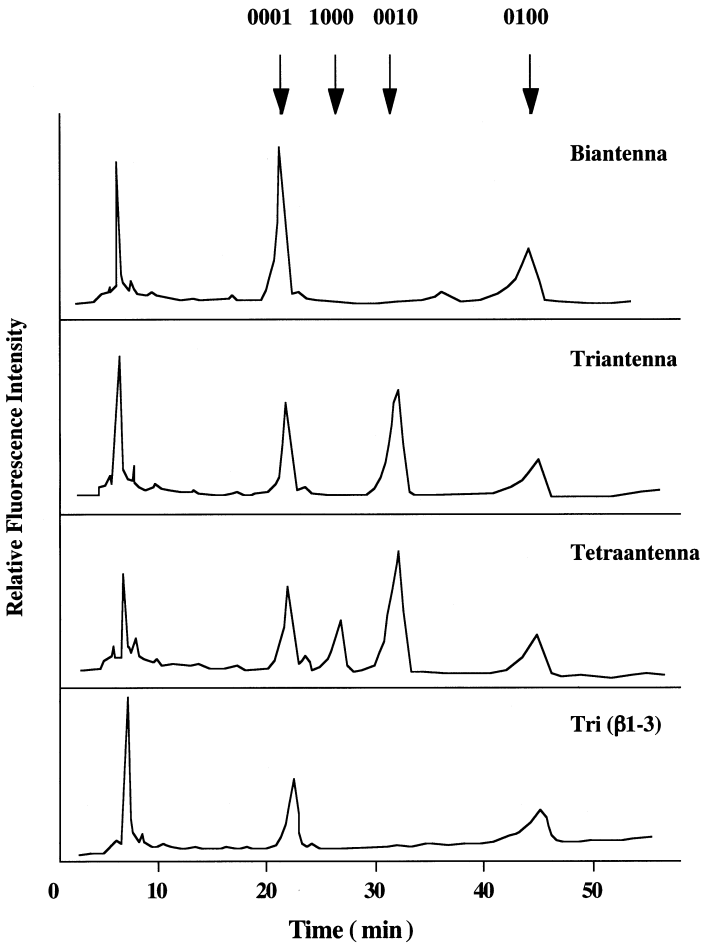

Figure 7. TaKaRa Palpak Type R reverse-phase chromatography. Various PA-oligosaccharides sugar chains, which had been incubated with GlcAT-P and UDP-[^{14}C]GlcA, were subjected to selective Branch Scission analysis as described under Materials and Methods, and then applied to a Takara Palpak Type R reverse phase column. Arrows indicate the elution positions of the standard PA-oligosaccharides listed in Figure 6.

0001, suggesting that GlcAT-P preferentially acts on *N*-acetyllactosamine on an αMan (1-3) arm. The most predominant substitution occurred on the αMan (1-3) branch, and 46 and 59 percent of the digestive products of tri- and tetra-antennary oligosaccharides were recovered as 0010, respectively, indicating that the Galβ1-4GlcNAcβ1-4Manα1-3 branch is the most potent acceptor of GlcAT-P. The molecular mechanism underlying this branch specificity is currently unclear. The enzyme could recognize the GlcNAcβ1-4Man linkage per se or the presence of other branches may influence the enzymic activity towards Galβ1-4GlcNAcβ1-4Manα1-3 branch. It should be noted that, when tri (β1-3)PA-oligosaccharide, which has a Galβ1-3GlcNAc in the most potent branch, was used as the acceptor for GlcAT-P, GlcA was not incorporated into this branch at all. In contrast to GlcAT-P, GlcAT-S(D) can transfer GlcA to both β1-4 and β1-3 linked Gal[20]. These results indicate that GlcAT-P is highly specific for the *N*-acetyllactosamine structure and transfers GlcA to the terminal galactose of *N*-acetyllactosamine residues, but the efficiency of this GlcA transfer differs significantly from branch to branch in *N*-glycans.

Discussion

In the present study, we examined the acceptor specificity of rat GlcAT-P associated with biosynthesis of the HNK-1 epitope on glycoproteins using ASOR and authentic PA-oligosaccharides as model acceptor substrates. We obtained the following evidence; 1) Structural analysis of oligosaccharides on ASOR, to which glucuronic acid was transferred, demonstrated that the GlcAT-P did not distinguish bi-, tri-, and tetra antennary *N*-glycans, and that all sugar chains almost equally served as acceptors. 2) The GlcAT-P transferred GlcA to non-reducing terminal *N*-acetylglucosamine branches with different efficiencies and utilized most preferentially the Galβ1-4GlcNAcβ1-4Manα1-3 branch as an acceptor, indicating that the GlcAT-P has so-called branch specificity. 3) The GlcAT-P specifically recognizes the terminal *N*-acetyllactosamine (Gal β1-4GlcNAc) structure, and the enzyme did not transfer GlcA to the Galβ1-3 residue linked to the GlcNAcβ1-4Manα1-3 branch at all.

Previously, Burger *et al.* characterized the *N*-linked oligosaccharide structures of human myelin-associated glycoprotein (MAG) and P0 by means of serial lectin affinity

Table 2. Branch specificity of GlcAT-P. Authentic PA-oligosaccharides listed in Figure 6 were incubated with GlcAT-P for 3 h. After collection of mono-GlcA-transferred oligosaccharides, GlcA-transferred branches were quantitated by the *Selective Branch Scission Method* (see Materials and methods)

	Percentage distributions of GlcA-transferred			
PA-oligosaccharides	*Biantenna*	*Triantenna*	*Tetraantenna*	*Tri-(β1-3)*
1000	–	–	15	–
0100	40	15	22	30
0010	–	59	46	0
0001	60	26	17	70

chromatography of the ^{14}C-labelled glycopeptides [26,27]. The HNK-1 epitope was carried by different types of *N*-linked oligosaccharides of MAG and P0. These results are coincident with our present results; the GlcAT-P transferred GlcA to the *N*-acetyllactosamine structures of all sugar chains including those of bi-, tri-, and tetra-antennary oligosaccharides on ASOR. They also indicated that the HNK-1 epitope was carried mainly by *N*-linked oligosaccharide structures α(1-6) fucosylated at the core [27]. In the present study, GlcA was more effectively transferred to triantennary oligosaccharides with α(1-6) fucose (Tri-Fuc) than to those without fucose (Triantenna) (see Table 1). However, the difference is so small that it is not clear whether or not the an α(1-6) fucose residue is a key residue recognized by GlcAT-P and for expression of the HNK-1 epitope.

The HNK-1 epitope is not expressed on all glycoproteins, being only expressed on a subset of glycoproteins, especially on cell adhesion molecules [4–7,28]. The present results indicate that the control mechanism for HNK-1 expression is not associated with the presence of a unique or uncommon carbohydrate commonly shared by these adhesion molecules. Furthermore, rat MAG has a total of eight potential *N*-linked glycosylation sites distributed amongst its five Ig-like domains [29,30]. These sites are located in rat MAG accordingly: one site in each of the first two Ig-like domains and two sites in each of the third, fourth, and fifth ones. Pedraza *et al.* demonstrated that the HNK-1 epitope is present on the fourth and/or fifth immunoglobulin domains of rat MAG [31]. These lines of evidence suggest that the activity of GlcAT-P may be modulated by some polypeptide determinant. Certainly, such polypeptide effects are seen as in the case of the high preference of polysialyltransferase for NCAM [32,33]. To address the question as to the regulation mechanism for HNK-1 epitope expression on some specific glycoproteins, we need further investigation on the acceptor specificity of GlcAT-P involving endogenous glycoprotein acceptors such as NCAM and MAG.

In the present study, we demonstrated that Galβ1-4GlcNAcβ1-4Manα1-3Man branch is the most potent acceptor of GlcAT-P. However, the structure of the HNK-1 carbohydrate epitope so far determined indicated that GlcA is transferred to Galβ1-4GlcNAcβ1-2Manα1-6Man branch (see Figure 1). This is simply because of the presence of a galactose residue in only this branch. The localization of the HNK-1 carbohydrate epitope will be determined by the availability of the galactose residue as an acceptor for GlcAT-P as well as the branch specificity of GlcAT-P.

It has been reported that several glycosyltransferases act preferentially on a defined branch of a multiple antennary oligosaccharide, so-called "branch specificity", including β(1-4)-galactosyltransferase [34], α(2-3)-sialyltransferase [35], and α(2-6)-sialyltransferase [36,37]. A survey on several *N*-glycoproteins, which contain both α2-3 and α2-6 linked sialic acid residues, showed that the Galβ1-4GlcNAcβ1-2Manα1-3Man branch generally carries a sialic acid through an α2-6 linkage, whereas the Galβ1-4GlcNAcβ1-4Manα1-3Man branch terminates with an α2-3-linked sialic acid [38]. These branch specificities of these sialyltransferases were confirmed by *in vitro* studies involving glycopeptides and oligosaccharides [35–38]. In the present study, we demonstrated that GlcAT-P exhibits similar branch specificity to α(2-3)-sialyltransferase. One of the functions of the HNK-1 carbohydrate is thought to be modulation of the properties of cell adhesion molecules. It should be noted, in connection with this, that the increase in the expression of the HNK-1 carbohydrate is correlated with the decrease in the polysialic acid content in the perinatal period in rat brain [3,16]. Therefore, GlcAT-P might compete for the Galβ1-4GlcNAcβ1-4Manα1-3Man branch with α2-3 sialyltransferase. It is known that the first sialic acid residue transferred to the potential polysialylation site of *N*-linked type sugar chains is α2-3 sialic acid [39]. If the sialic acid is substituted by GlcA in situ, then the polysialic acid chains would not be formed. In fact, it has been reported that overexpression of a β-galactoside α2-6 sialyltransferase in Xenopus embryos blocks the synthesis of PSA [40]. Our preliminary results indicate that the HNK-1 epitope on rat NCAM is expressed at least in the fifth Ig domain (unpublished observation), to which polysialic acid is known to attach [32,41]. These lines of evidence suggest that expression of the HNK-1 epitope on NCAM may modulate PSA expression and regulate the adhesive properties of NCAM.

Acknowledgements

We would like to thank Ms T. Honda & N. Nishigaki for their secretarial assistance. This work was supported in part by a Grant-in-Aid for Scientific Research (A-09307053), a Grant-in Aid for Scientific Research (C-11680604) from the Japan Society for the Promotion of Sciences, and a Grant-in-Aid for Scientific Research on Priority Areas (A-10178104) from the Ministry of Education, Science, Sports and Culture of Japan.

References

1 Abo T, Balch CM, *J Immunol* **127**, 1024–9 (1981)
2 Schwarting GA, Jungalwala FB, Chou DK, Boyer AM, Yamamoto M, *Dev Biol* **120**, 65–76 (1987).
3 Yoshihara Y, Oka S, Watanabe Y, Mori K, *J Cell Biol* **115**, 731–44 (1991).
4 Kruse J, Mailhammer R, Wernecke H, Faissner A, Sommer I, Goridis C, Schachner M, *Nature* **311**, 153–5 (1984).
5 McGarry RC, Helfand SL, Quarles RH, Roder JC, *Nature* **306**, 376–8 (1983).
6 Dodd J, Morton SB, Karagogeos D, Yamamoto M, Jessell TM, *Neuron* **1**, 105–16 (1988).
7 Krueger R Jr, Hennig AK, Schwartz NB, *J Biol Chem* **267**, 12 149–61 (1992).
8 Künemund V, Jungalwala FB, Fischer G, Chou DK, Keilhauer G, Schachner M, *J Cell Biol* **106**, 213–23 (1988).
9 Bronner-Fraser M, *Dev Biol* **123**, 321–31 (1987).
10 Martini R, Xin Y, Schumitz B, Schachner M, *Eur J Neurosci* **4**, 628–39 (1992).
11 Ilyas AA, Quarles RH, Brady RO, *Biochem Biophys Res Commun* **122**, 1206–11 (1984).
12 Chou DK, Ilyas AA, Evans JE, Costello C, Quarles RH, Jungalwala FB, *J Biol Chem* **261**, 11 717–25 (1986).
13 Ariga T, Kohriyama T, Freddo L, Latov N, Saito M, Kon K, Ando S, Suzuki M, Hemling ME, Rinehart K Jr, *J Biol Chem* **262**, 848–53 (1987).
14 Voshol H, van-Zuylen CW, Orberger G, Vliegenthart JF, Schachner M, *J Biol Chem* **271**, 22 957–60 (1996).
15 Oka S, Terayama K, Kawashima C, Kawasaki T, *J Biol Chem* **267**, 22 711–4 (1992).
16 Kawashima C, Terayama K, Ii M, Oka S, Kawasaki T, *Glycoconj J* **9**, 307–14 (1992).
17 Terayama K, Nakamura A, Seiki T, Matsumori K, Ohta S, Oka S, Sugita M, Kawasaki T, *J Biol Chem* **273**, 30 295–300 (1998).
18 Terayama K, Oka S, Seiki T, Miki Y, Nakamura A, Takio K, Kozutsumi Y, Kawasaki T, *Proc Natl Acad Sci USA* **94**, 6093–98 (1997).
19 Seiki T, Oka S, Terayama K, Imiya K, Kawasaki T, *Biochem Biophys Res Commun* **255**, 182–7 (1999).
20 Shimoda Y, Tajima Y, Nagase T, Harii K, Osumi N, Sanai Y. *J Biol Chem* **274**, 17 115–22 (1999).
21 Tone Y, Kitagawa H, Imiya K, Oka S, Kawasaki T, Sugahara K, *FEBS Lett* **459**, 415–20 (1999).
22 Wei G, Bai X, Sarkar AK, Esko JD, *J Biol Chem* **274**, 7857–64 (1999).
23 Yoshima H, Matsumoto A, Mizuochi T, Kawasaki T, Kobata A, *J Biol Chem* **256**, 8476–84 (1981).
24 Kitamura K, Uyemura K, Shibuya K, Sakamoto Y, Yoshimura K, Nomura M, *J Neurochem* **75**, 853–60 (2000).
25 Fournet B, Montreuil J, Strecker G, Dorland L, Haverkamp J, Vliegenthart FG, Binette JP, Schmid K, *Biochemistry* **17**, 5206–14 (1978).
26 Burger D, Simon M, Perruisseau G, Steck AJ, *J Neurochem* **54**, 1569–75 (1990).
27 Burger D, Perruisseau G, Simon M, Steck AJ, *J Neurochem* **58**, 854–61 (1992).
28 Yoshihara Y, Oka S, Ikeda J, Mori K, *Neurosci Res* **10**, 83–105 (1991).
29 Arquint M, Roder J, Chia LS, Down J, Wilkinson D, Bayley H, Braun P, Dunn R, *Proc Natl Acad Sci USA* **84**, 600–4 (1987).
30 Salzer JL, Holmes WP, Colman DR, *J Cell Biol* **104**, 957–65 (1987).
31 Pedraza L, Spagnol G, Latov N, Salzer JL, *J Neurosci Res* **40**, 716–27 (1995).
32 Nelson RW, Bates PA, Rutishauser U, *J Biol Chem* **270**, 17 171–9 (1995).
33 Kojima N, Tachida Y, Yoshida Y, Tsuji S, *J Biol Chem* **271**, 19 457–63 (1996).
34 Blanken WM, van-Vliet A, van-den-Eijnden DH, *J Biol Chem* **259**, 15 131–5 (1984).
35 Nemansky M, van-den-Eijnden DH, *Glycoconj J* **10**, 99–108 (1993).
36 Joziasse DH, Schiphorst WE, van-den-Eijnden DH, van-Kuik JA, van-Halbeek H, Vliegenthart JF, *J Biol Chem* **260**, 714–9, (1985).
37 Nemansky M, Edzes HT, Wijnands RA, van-den-Eijnden DH, *Glycobiology* **2**, 109–17 (1992).
38 Joziasse DH, Schiphorst WE, van-den-Eijnden DH, Van-Kuik JA, Van-Halbeek H, Vliegenthart JF, *J Biol Chem* **262**, 2025–33 (1987).
39 Finne J *J Biol Chem* **257**, 11 966–70 (1982).
40 Livingston BD, De-Robertis EM, Paulson JC, *Glycobiology* **1**, 39–44 (1990).
41 Crossin KL, Edelman GM, Cunningham BA, *J Cell Biol* **99**, 1848–55 (1984).

Received 28 September 2000, revised 5 April 2001,
accepted 6 April 2001